MULTI-SCALE STRUCTURES ASSOCIATED WITH IGNEOUS INTRUSIONS AND IMPLICATIONS FOR FLUID MIGRATIONS – A REVIEW OF RECENT RESEARCH

Olivier Galland[1], Hernán de la Cal[2], José Mescua[3], Ole Rabbel[1], Frank Guldstrand[1], Dougal Jerram[4,5]

1: The NJORD Centre, Department of Geosciences, University of Oslo, Norway. olivier.galland@geo.uio.no

2: ROCH S.A., Buenos Aires, Argentina. hdelacal@roch.com.ar

3: Instituto Argentino de Nivología, Glaciología y Ciencias Ambientales. CCT Mendoza, CONICET; y Facultad de Ciencias Exactas y Naturales, Universidad Nacional de Cuyo, Mendoza, Argentina. jmescua04@yahoo.com.ar

4: Centre for Earth Evolution and Dynamics (CEED), University of Oslo, Norway

5: DougalEARTH Ltd., UK. dougal@dougalearth.com

Keywords: Igneous Intrusions, Emplacement Processes, Structures, Fracture, Dome, Permeability

RESUMEN

Los intrusivos ígneos juegan un papel importante en la maduración, migración y entrampamiento de hidrocarburos. La Cuenca Neuquina, por ejemplo, alberga varios yacimientos productores de hidrocarburos que están directamente asociados a estas rocas. La última década de investigación se concentró en el impacto térmico de estas intrusiones. Esta contribución tiene como objetivo demostrar que los intrusivos también tienen impacto estructural significativo a diferentes escalas en las secuencias sedimentarias donde se emplazan, con implicancias de primer orden para el flujo y entrampamiento de fluidos, utilizando ejemplos de la Cuenca Neuquina. En primer lugar, a pequeña escala, el emplazamiento del magma produce la fractura y daño de las rocas de caja. Se presentarán observaciones estructurales detalladas de campo de filones expuestos en Las Loicas. Allí, tanto los filones como las estructuras en la roca de caja se pueden mapear en detalle, destacándose cómo las fracturas y el daño están controlados por la forma de las intrusiones, es decir, steps y puntas. Estas observaciones están respaldadas por modelos de laboratorio bidimensionales cuantitativos del emplazamiento del magma en la corteza frágil. En segundo lugar, a gran escala, el emplazamiento de intrusiones tabulares como filones y lacolitos provocan el domamiento de las capas suprayacentes: si el domo es suave, la estructura puede ser una buena trampa, mientras que un domo más prominente puede conducir a fallamiento y, por lo tanto, a la fuga de fluidos o desarrollo de un yacimiento fracturado. Se presentarán los resultados del estudio del lacolito Pampa Amarilla, y se mostrará cómo la integración de observaciones de campo, datos de pozos y sísmica es crucial para una caracterización estructural adecuada del domo inducido por el lacolito. Además, los modelos de laboratorio de emplazamiento de magma muestran cómo la forma de la intrusión controla el estilo estructural del domo asociado. Finalmente, la deformación frágil dentro de las rocas ígneas asociada a su emplazamiento, también puede desempeñar un papel fundamental en la migración de fluidos. Se reportarán observaciones de campo del Cerro Alquitrán (domo andesítico), en cuyo borde se observa un manadero de petróleo. El mapeo de campo muestra que la migración del petróleo está controlada por brechas y bandas de fractura que resultan de la deformación frágil del magma durante su emplazamiento. Estos estudios integrados de campo y modelado muestran que una comprensión profunda de las implicancias estructurales de las intrusiones ígneas es crucial para la evaluación de los sistemas petroleros en cuencas volcánicas.

INTRODUCTION

Igneous intrusions emplaced in sedimentary basins play a major role for hydrocarbon maturation, migration and trap (Senger *et al.* 2017, and references therein). The main known effects of igneous intrusions petroleum systems are: (1) increasing thermal maturity of organic-rich host rocks and stimulating hydrocarbon generation, (2) inducing fractures in response to the circulation of over-pressurized, hydrothermal fluids, which can act as migration pathways for fluid flow, (3) forming hydrothermal vents systems that can release these fluids to the atmosphere, and (4) forming structures induced by the emplacement process, such as forced-folds, that can act as hydrocarbon traps.

The Neuquén basin hosts several producing oil and gas fields that are directly associated with subsurface igneous intrusions (González and Aragón 2000; Comeron *et al.* 2002; Bermúdez and Delpino 2008; Rodriguez Monreal *et al.* 2009; Witte *et al.* 2012; Schiuma and Llambías 2014; Fuentes *et al.* 2016; de la Cal *et al.* 2018; Spacapan *et al.* 2020). Hydrocarbon fields in other Argentinian basins also appear to be affected by igneous intrusions (Plazibat *et al.* 2019). The last decade of research has mostly focused on the thermal impacts of igneous intrusions, especially the contact metamorphism induced by sills emplaced in organic-rich shale formations (Spacapan *et al.* 2018). However, recent research also highlights the first-order structural implications of igneous intrusions on fluid flow, and in particular on hydrocarbon systems, at different scales. The aim of this contribution is to provide a brief multidisciplinary review of our understanding of the structural impacts of igneous intrusions on petroleum systems (Fig. 1).

This review paper is organized in the following structure:

- In a first section, we describe small-scale (tip-scale) structural impacts of igneous intrusions on the surrounding sedimentary rock formations.
- In a second section, we describe large-scale (intrusion-scale) structural impacts of igneous intrusions on the surrounding sedimentary rock formations.
- In a third section, we describe how structures within igneous intrusions play a major role on fluid flow.
- Finally, in a fourth section, we list the fracturing processes that develop in igneous complexes emplaced in organic-rich shale, both within the intrusions and the metamorphic aureoles.

SMALL-SCALE STRUCTURAL IMPACTS OF IGNEOUS INTRUSIONS

Magma propagates in a forceful manner, such that magma propagations occurs by damaging and failing the host rock (Fig. 1A). This process is expected to produce numerous fractures and structures in the near vicinity of igneous intrusions, which can have significant impacts on fluid flow. Understanding the distribution, density and connectivity of these small-scale structures, and

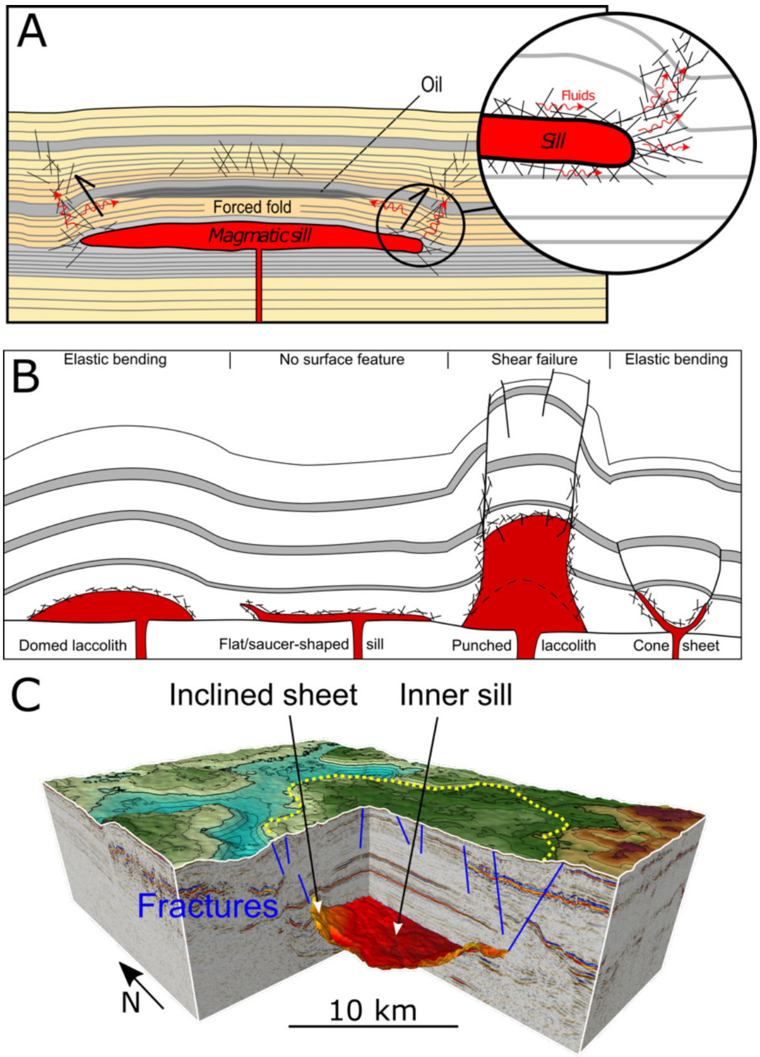

Figure 1. Examples illustrating the structural implications of igneous intrusions on their host rock. A. Schematic drawing of igneous sill and mechanical implications on sedimentary host rock. Intrusion-scale doming, or forced folds, can be hydrocarbon traps, whereas small-scale fractures and damage can be fluid pathways. B. Schematic drawing of various degrees of overburden deformation associated thin sills, domes laccoliths and punched laccoliths. Modified from Delpino *et al.* (2014). C. 3D seismic block of the Tulipan sill and the associated structures in its overburden, Møre Basin, offshore Norway. From Schmiedel *et al.* (2017b).

their fluid flow implications, require a solid knowledge of the propagation mechanisms of the intrusion.

Igneous sheet and tabular intrusions, such as dykes, sills and laccoliths, are the most fundamental igneous bodies observed in sedimentary basins (Petford *et al.* 2000; Cartwright and Hansen 2006; Magee *et al.* 2016; Galland *et al.* 2018). In particular, the last two decades of research have highlighted that voluminous sill complexes accommodate extensive lateral and vertical magma transport and emplacement in sedimentary basins worldwide (Magee *et al.* 2016; Galland *et al.* 2018). Most mechanical models of sill emplacement consider sills and laccoliths

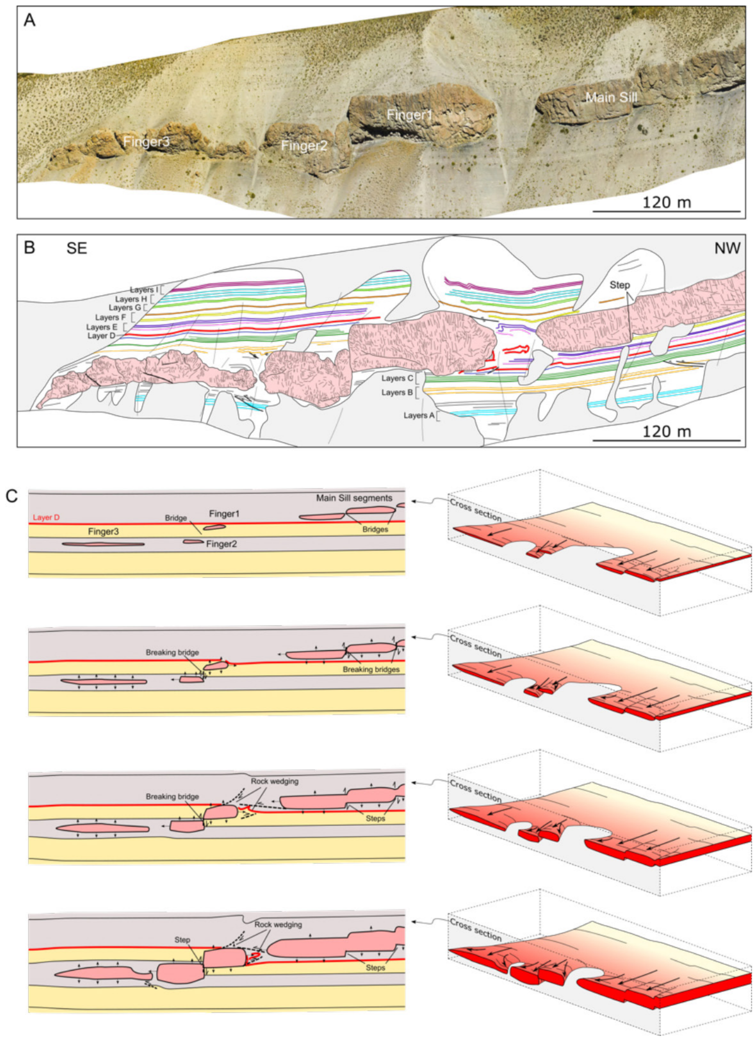

Figure 2. A. Orthorectified image of outcrop studied at Las Loicas, Mendoza province, computed using 126 drone photographs. B. Structural interpretation of orthorectified image of A. Faults are indicated as bold black lines. C. Schematic 3D block diagram (right) and corresponding cross sections (left) drawings of the emplacement scenario of the sill and fingers and associated damage at La Loicas, Mendoza province. From Galland *et al.* (2019).

as continuous igneous sheets, emplacing and propagating as hydraulic fractures (Pollard 1973; Bunger and Cruden 2011; Galland and Scheibert 2013). These models assume that the host rock behaves as a purely elastic medium, and that there is a single peripheral propagating edge. However, in many basins, igneous sills are preferentially emplaced into formations of certain lithologies, often shale (Rossello *et al.* 2002; Rodriguez Monreal *et al.* 2009; Witte *et al.* 2012; Spacapan *et al.* 2018), which exhibit inelastic behaviours (Pollard *et al.* 1975; Schofield *et al.* 2012; Wilson *et al.* 2016; Spacapan *et al.* 2017). This strongly questions the applicability of the purely elastic models to address the emplacement of sills in weak rock formations, particularly in shale (Scheibert *et al.* 2017). Addressing the structural consequences of igneous intrusions requires (1) detailed geological observations from well-exposed intrusions and their host rock, and (2) models that account for inelastic properties of the host rock.

Field observations: the Las Loicas (southern Mendoza province) case study

Galland *et al.* (2019) presented results of detailed structural mapping of an exceptional, easily accessible 1-km long outcrop at Las Loicas, located in the Neuquén Basin, Argentina (Figure 2), which exhibits a sill composed of a string of igneous fingers, their contacts and the structures in the finely layered sedimentary host rock. This outcrop (1) reveals how the host rock accommodates the emplacement of the fingers, and (2) provides direct structural evidence of magma flow direction through the studied fingers.

The conclusions of Galland *et al.* (2019)'s study are (see Figure 2): (1) The sill is made of segments emplaced at distinct stratigraphic levels. These segments subsequently grew, either inflating to distinct fingers, or coalescing to a stepped sill. (2) Sharp vertical contacts between fingers could incorrectly be interpreted as tectonic fault offsets, however Galland *et al.* (2019) demonstrate that they are in fact primary emplacement features and result from the coalescence of fingers. (3) The segmented nature of the intrusion shows that its overall sheet shape does not result from the emplacement of a single sheet, as assumed by most models, but from the coalescence of fingers. (4) The edges of the fingers are blunt and their propagation occurred by pushing aside the host rock, leading to intense shortening, rock wedging, and even squeezing of the host rock in between the fingers. This shows that the inelastic properties of crustal rocks are of primary importance on the emplacement of magma intrusions in the shallow brittle crust. (5) These small-scale structural observations carried out on a seismic-scale outcrop should considerably aid the structural interpretation of seismic imaging of igneous sills, filling the gap between outcrop-scale field observations and seismic-scale geophysical data.

2-dimensional laboratory modelling

2D laboratory experiments have been designed to map and quantify the damage induced by propagating igneous intrusions (Abdelmalak *et al.* 2012; Guldstrand *et al.* submitted). In particular, these studies aim at assessing how the host rock's brittle properties affect damage distribution.

Host rock consists of 4 different mixes of silica flour (SF) and glass microbeads (GB) (Guldstrand *et al.*, submitted). These two fine-grained materials fail according to a Mohr-Coulomb criterion (Abdelmalak *et al.* 2016). The GB flour is nearly cohesionless as it collapses under its own weight. SF is cohesive when compacted: it does not collapse under its own weight and sustains vertical walls (Galland *et al.* 2006). Abdelmalak *et al.* (2016) showed that the cohesion of GB/SF mixes follows a near linear trend with respect to mixing proportion, so that these mixes allow us

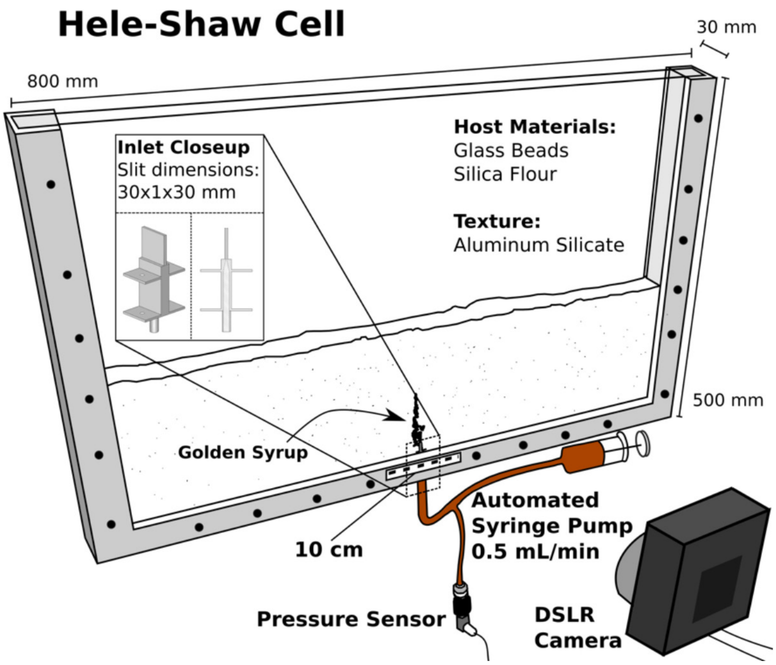

Figure 3. Drawing of the 2D experimental setup to model magma emplacement in the brittle crust. From Guldstrand *et al.* (submitted).

to explore the effect of variable cohesion on the modeled processes. The magma analogue was glucose syrup (Golden Syrup in Norway) of viscosity ~55 Pa s and density ~1440 kg m-3 at 21°C. The experimental setup consists of a thick 2D hele-shaw cell with dimensions 80 cm wide, 50 cm high and 3 cm thick (Fig.3). An interchangeable inlet is placed at the bottom of the cell to inject the Golden Syrup. The viscous Golden Syrup was put into a syringe, which was then put into a syringe pump and connected to the inlet with a T-connector in-between pump and inlet. The experiments were done at constant flow rate of 0.5 ml min-1 for all experiments.

The emplacement of the Golden Syrup in the models was observable from the sides through the glass plates, and monitored using a DSLR camera. Digital image correlation between successive images was implemented to compute displacement maps in the host. Shear strain maps are subsequently calculated to highlight the development of small-scale structures associated with the propagation of the Golden Syrup, highlighting the incremental evolution of inelastic damage in relation to syrup propagation (Fig. 4).

The main conclusions are (see Figure 4): (1) Continuous sheet intrusions form in high-cohesion hosts, whereas discontinuous finger-shaped intrusions form in low-cohesion hosts; (2) In all experiments, inelastic shear damage with, and uplift of, the host accommodate partly the emplacement of the model magma; (3) Sheet intrusions in high-cohesion hosts grow dominantly by dilation and opening along the entire length of the intrusion. In contrast, finger-shaped intrusions only thicken near the propagating tip of the intrusion; (4) The propagation

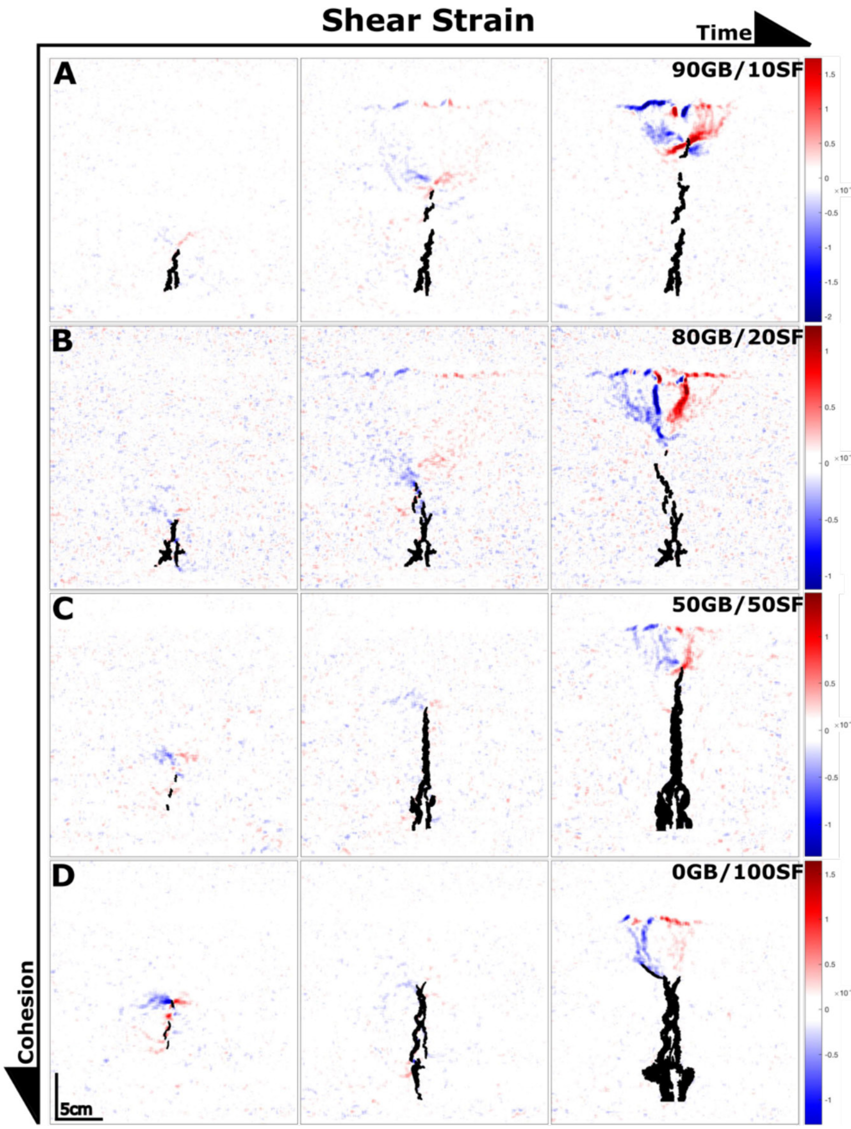

Figure 4. Shear strain maps monitored during 2D experiments of magma emplacement. The rows show intrusions (black) into mixes of 90/10 (A), 80/20 (B), 50/50 (C) and 0/100 (D). Columns show experiment photos at an initial, intermediate and late time step. The computed shear strain in A and B extends from the intrusion already at depth until ultimately causing critical failure of the overburden. C & D show smaller zones of shear associated with the intrusion tip. The scale has been adjusted to enhance smaller shear strains at depth. From Guldstrand *et al.* (submitted).

of the fingers' tips is accommodated by significant shear damage bands, showing that the fingers dominantly propagate by pushing their host rock ahead, in agreement with the so-called viscous indenter model. Conversely, shear damage is much less prominent near the tip of sheet intrusions, which dominantly propagate like fractures; (5) All in all, the experiments shows that intrusion-induced damage distribution strongly differs depending on the magma emplacement mechanism.

LARGE-SCALE STRUCTURAL IMPACTS OF IGNEOUS INTRUSIONS

The emplacement of sills and laccoliths leads to the formation of dome-structures (Trude *et al.* 2003; Magee *et al.* 2014; Agirrezabala 2015), which can have tremendous implications for fluid trap (Orchuela *et al.* 2003). The mechanisms controlling magma accumulation and overburden doming, and so the resulting structures within the dome, depend to a great extent on the deformation mechanism of the overburden (Fig. 1B)(Corry 1988). Assessing whether sill- or laccolith-induced domes act as traps, fractured reservoirs or leaks relies on understanding the mechanics of sill and laccolith fluid emplacement.

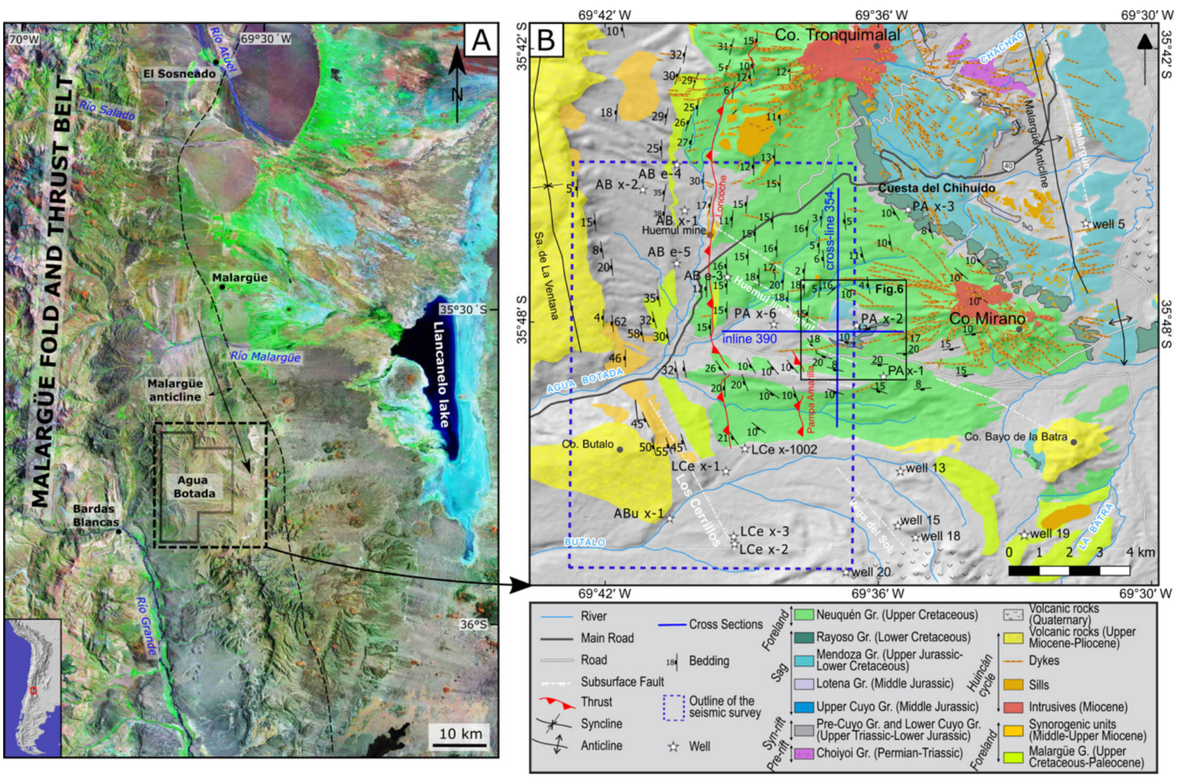

Figure 5. A. Satellite image locating the study area including the Agua Botada block (black solid lines polygon) and surroundings main structures (base image is a LANDSAT7+ satellite image (RGB741 band combination)). Black dashed rectangle locates map of B. Modified from (Barrionuevo *et al.* 2019). B. Main geologic units and structures in the Agua Botada area. Modified from Barrionuevo *et al.* (2019). Blue dashed rectangle locates 3D seismic survey used in this study. Black box locates the detailed geological map of Figure 6. Blue segments locate geological cross sections of Figure 7.

One end-member model of laccolith-induced doming is based on the elastic bending of overlying strata, which are considered as a thin, stiff plate (Pollard and Johnson 1973). This model end-member is widely implemented, as the mathematical formulation of a thin, stiff bending plate is relatively easy. This model end-member formulation is valid only for very shallow laccoliths (depth-to-diameter ratio $H/D<0.1$) with low thickness-to-diameter aspect ratios of the intrusions

(T/D<0.02) (Ventsel and Krauthammer 2002). However, most laccoliths documented on Earth do not fulfil these geometrical conditions (Corry 1988; Cruden *et al.* 2018), as most laccoliths exhibit higher values of H/D, and some intrusions are almost as thick as they are wide (Jackson and Pollard 1990; Rodriguez Monreal *et al.* 2009; Mattsson *et al.* 2018). In addition, field observations show that significant fracturing and faulting (i.e., inelastic deformation) can accommodate doming of laccolith overburdens (Wilson *et al.* 2016; Mattsson *et al.* 2018), as accounted for in the end-member "punched laccolith" model where the overburden lifts up like a rigid piston (Corry 1988; Schmiedel *et al.* 2019).

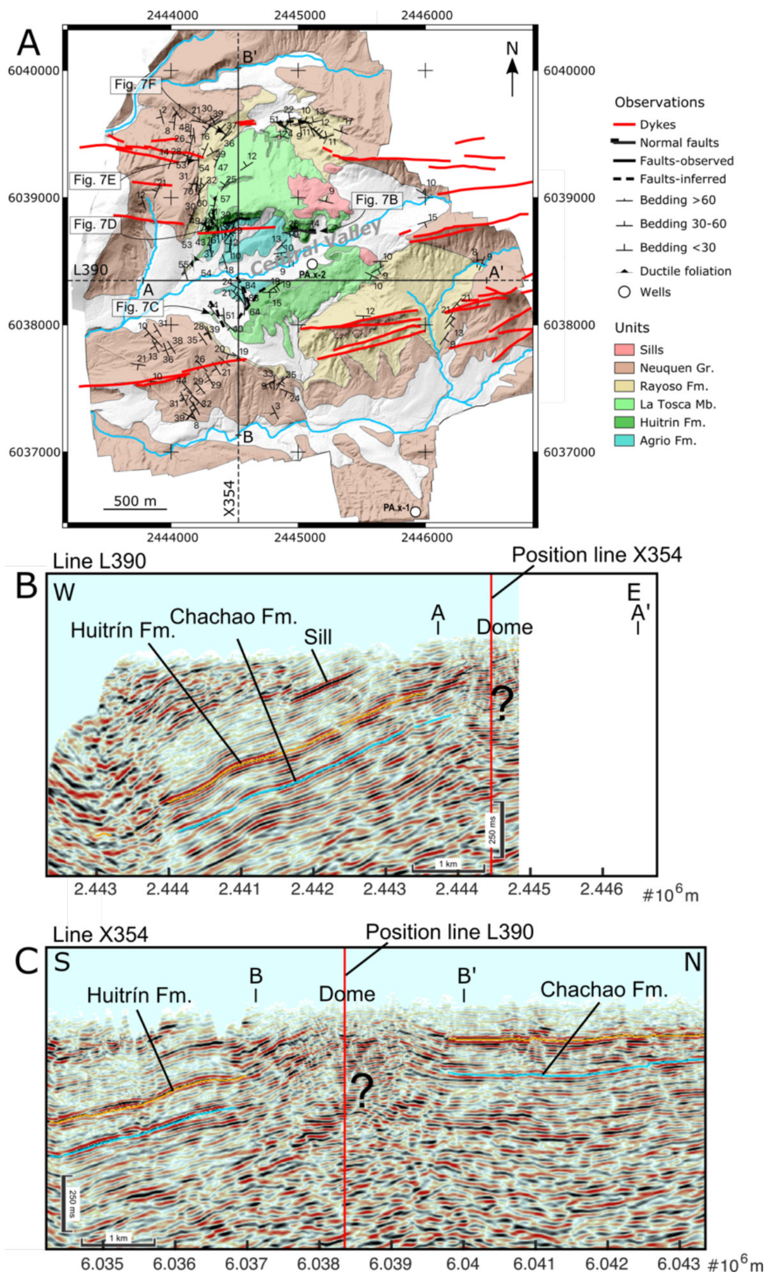

Figure 6. A. Geological map of the Pampa Amarilla dome (see location in Figure 5) showing structural field measurements, seismic profiles (see B and C) and geological cross sections (Fig. 7). Topography data were calculated from photogrammetric drone surveys. The coordinate system of the map is the Campo Inchauspe / Argentina 2 EPSG:22192. B and C. Examples of seismic profiles across the Pampa Amarilla dome (see locations on Figure 5) with interpreted tops of the Huitrín (orange lines) and Chachao (light blue lines) formations. B. W-E profile showing a gently-dipping monoclinal structure. A forced fold is located on the eastern edge of the profile, where the seismic data is incoherent. C. NS profile showing a gently-dipping monoclinal structure to the south and horizontal layering to the north. A forced fold occurs in the middle of the profile, where the seismic data is incoherent. It is impossible to reconstruct the structure of the dome and the shape and extent of the underlying intrusion on both the EW and NS lines. From Galland *et al.* (2022).

Field observations: Pampa Amarilla (southern Mendoza province) case study

Galland *et al.* (2022) describe the detail structure of a laccolith-induced dome by integrating geological field mapping, 3D seismic data and borehole data. This case study is the Pampa Amarilla dome structure, located in the Malargüe fold-and-thrust belt in the northern Neuquén Basin, southern Mendoza province, Argentina, ~50 km to the south of the town of Malargüe and 20 km to the east of the village of Bardas Blancas (Fig. 5). A thick igneous body at Pampa Amarilla, in the Agua Botada area, has been known since 1937 after the drilling of well PA.x-2, which crossed ~100 meters of andesite without reaching the bottom of the intrusion. Barrionuevo *et al.* (2019) proposed that doming of Neuquén basin strata at Pampa Amarilla was the result of the intrusion of the andesite found in well PA.x-2.

Galland *et al.* (2022) completed detailed field structural mapping of the Pampa Amarilla dome, which intersects the thin Mesozoic Huitrín and Rayoso Fms. of the Neuquén Basin, in addition to the uppermost Agrio Fm. and the lowermost Neuquén Gr. (Fig. 5). The level of exposure and outcrop quality allowed to map several stratigraphic contacts almost continuously: Top Agrio Fm./base Huitrín Fm., Huitrín gypsum/La Tosca Mb., Top La Tosca Mb./base Rayoso Fm., and Top Rayoso Fm./base Neuquén Gr.

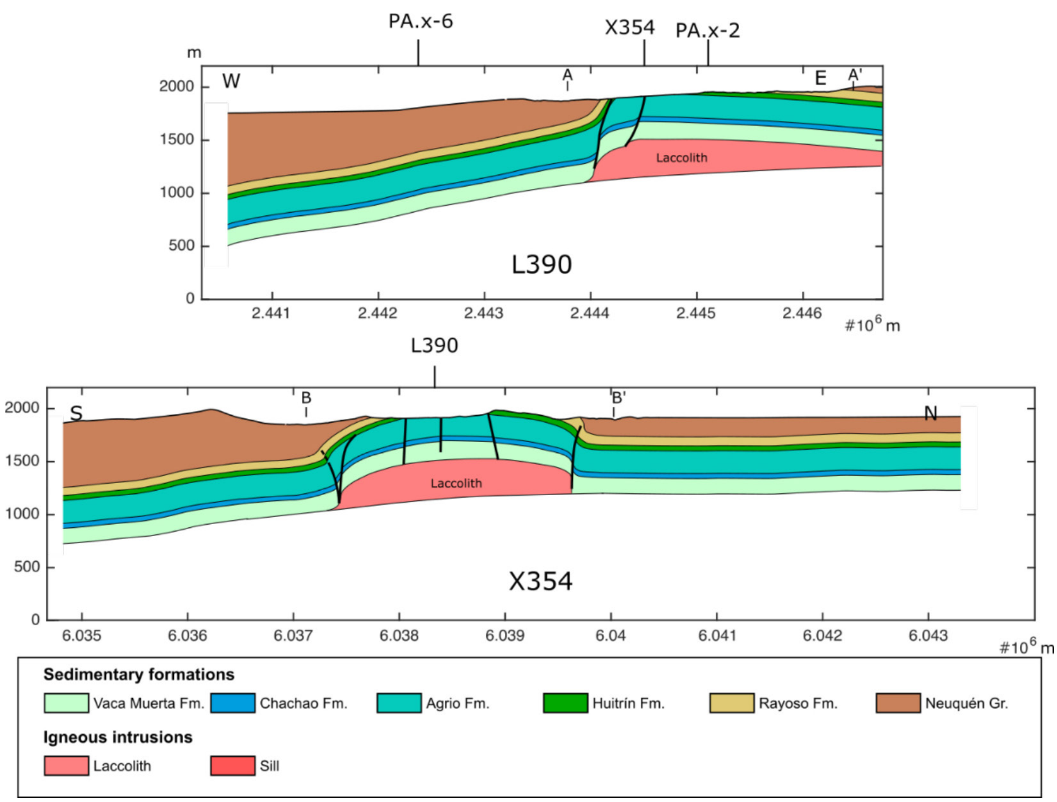

Figure 7. Cross sections of Pampa Amarilla dome and laccolith. Cross sections are located on Figure 5B. Segments of the cross sections A-A' and B-B' are located on geological map of Figure 6. The locations of wells PA.x-2 and PA.x-6 are indicated on Profile L390. The locations of the intersections with other cross sections are indicated on each profile. From Galland *et al.* (2022).

The study of Galland *et al.* (2022) integrates surface geological observations with subsurface 3D seismic and well data (Figure 6). The conclusions of this study are: (1) The Pampa Amarilla dome formed due to the emplacement of a ~400 m thick subsurface laccolithic intrusion, with a thickness-to-length ratio T/D~0.13. (2) The dome exhibits a trapdoor structure, with faulting along the western, northwestern and southerwestern edges, and gentle tilting of the overburden to the east. The trapdoor tilting of the laccolith's overburden was the main mechanism that controlled the thickening of the laccolith. (3) Minor faulting in the centre of the dome is attributed to 3D stretching of the overburden. (4) The reconstructed subsurface Pampa Amarilla laccolith is elliptical in map view, with a 3 km-long E-W axis and a 2 km-long N-S axis. Along E-W cross section, the laccolith is wedge shaped with maximum thickness near its western edge, and exhibits gradual thinning toward the east.

Given that numerous laccolithic intrusions exhibit similar values of T/D to that of Pampa Amarilla laccolith, the study of Galland *et al.* (2022) suggests that numerous laccoliths on Earth grew by faulting of their overburden. This result implies that the established mechanical models of laccolith emplacement based on elastic bending of the overburden may apply only to few, thin laccoliths/thick sills. Finally, this study highlights the necessity and value of integrating field geological measurements with subsurface 3D seismic and borehole data for structural reconstructions of subsurface laccolith intrusions.

3-dimensional laboratory modelling

The 3D experimental method is similar to that presented by Schmiedel *et al.* (2017a). The model rock and model consist of dry Mohr-Coulomb granular materials of variable cohesion (Galland *et al.* 2006; Abdelmalak *et al.* 2016), and molten vegetable oil, respectively (Fig. 8). Similarly to the 2-dimensional experiments described above, the granular materials used in this study consist of a mix of (1) a high cohesion fine-grained crystalline silica flour (SF; cohesion of ~600 Pa), and (2) a low cohesion micro glass beads (GB; cohesion of ~100 Pa; Fig. 8). These granular mixtures simulate a wide range of brittle rocks, from strong, competent rocks (e.g. limestone) to weak rocks (e.g. shale). A flexible net located within the granular material just above the inlet simulates a rock layer (Fig. 8). In these experiments, the model magma (vegetable oil) is injected at a constant volumetric flow rate Q of 40 ml min-1 (= 5.1 10-7 m3 s-1). Because the net is located just at the inlet (Fig. 8B), the oil directly flows horizontally along the flexible net to form a sill before propagating upwards.

The experiments produced variable intrusion geometries with varying experimental parameters. In high cohesion experiments, the intrusions were typical thin saucer-shaped intrusions, with circular, flat, horizontal inner sill and outer inclined sheets (Fig. 8C). In contrast, in low cohesion

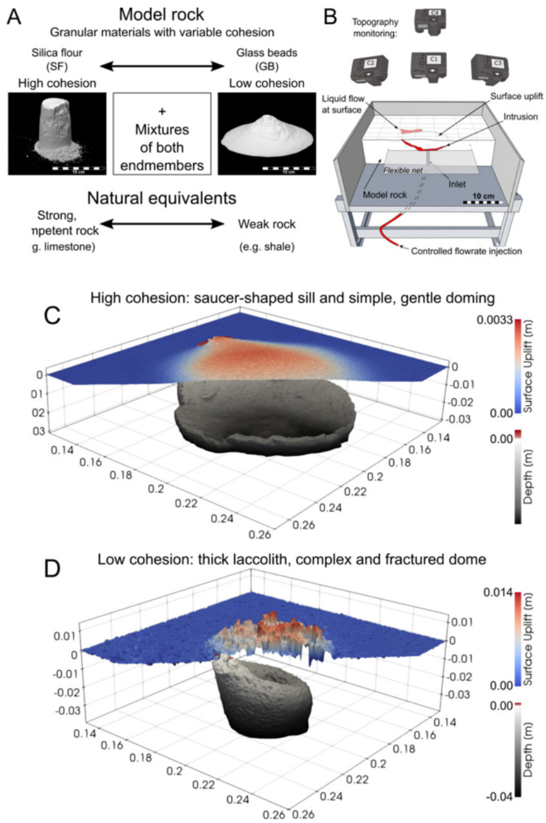

Figure 8. A. Photographs of granular materials used to model brittle rocks. Left: high cohesion, fine-grained crystalline silica flour to model competent rocks. Right: low cohesion, fine-grained glass beads to model loose rocks. B. Drawing of the 3D experimental setup to model magma emplacement in the brittle crust. Four synchronized cameras monitor the evolution of the model surface. C. Block diagram plotting digital elevation model (DEM) (colour) of model surface and underlying saucer-shaped intrusion from a characteristic 3D experiment in a high-cohesion experiment. The DEM evidences low amplitude, smooth uplift above the intrusion. D. Block diagram plotting digital elevation model (DEM) (colour) of model surface and underlying saucer-shaped intrusion from a characteristic 3D experiment in a low-cohesion experiment. The DEM evidence high amplitude, blocky uplift above the intrusion. From Schmiedel *et al.* (2019).

experiments, the intrusions were massive, piston-like intrusions, with sub-vertical sidewalls (Fig. 8C). Finally, in experiments with intermediate cohesions, the intrusions exhibit mostly inclined sheets, with a sub-horizontal bottom intrusion of radius smaller than those of intrusions emplaced in the high-cohesion experiments (Schmiedel *et al.* 2017a). The sheets in intermediate-cohesion experiments appear thicker than those in the high-cohesion experiments.

An important aspect of the trapping properties of forced folds induced by igneous sills and laccoliths is fracture development. Visual observation on orthorectified images of the model surfaces highlights the formation of surface discontinuities, i.e. fractures (Fig. 8C) (Schmiedel *et al.* 2019). In the middle of the uplifted area, a few open, dilating cracks are clearly visible, while at the edges of the uplifted area fractures accommodating shortening are visible (Fig. 8C). Such a fracture pattern is compatible with stress distribution across a dome induced by a shallow intrusion (e.g. Pollard and Johnson 1973; Galland and Scheibert 2013).

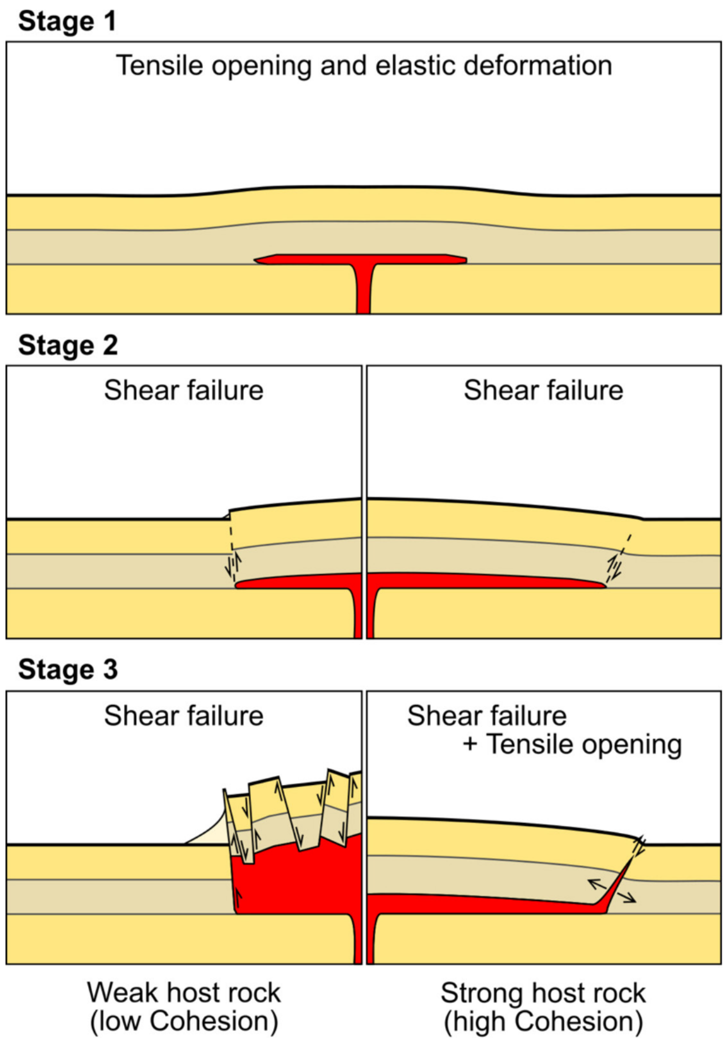

Figure 9. Schematic drawing of the two-stage evolution for horizontal igneous intrusions depending on the failure mode of the host rock. Left: scenario for a low cohesion overburden. Right: scenario for a higher cohesion overburden. From Schmiedel *et al.* (2019).

These models are the first able to address the inelastic damage and fracture patterns accommodating the emplacement of igneous intrusions in sedimentary sequences. In particular, they show that intrusions of distinct morphologies are associated with domes of very distinct structures. The models also show that even thin sills can trigger significant inelastic damage, and so potential fluid pathways. These results thus bring essential new geomechanical insights with respect to classic elastic models of magma emplacement, which and are unable to model and predict the inelastic damage and fractures observed in the field.

Another key question arising from Schmiedel *et al.* (2017a)'s experiments is: what are the processes that lead to drastically distinct final intrusion morphologies, and in particular the thickness-to-diameter (T/D) aspect ratio? The main variable parameter in Schmiedel *et al.*

(2017a)'s experiments is the Mohr-Coulomb properties of the intrusion's overburden: the higher the cohesion, the lower T/D, and so the thinner the intrusion appears. What about the magma viscosity? Schmiedel *et al.* (2019) derived a simple analytical model to address the effect of magma viscosity. They argue that the growth of a tabular intrusion results from the balance between the energy dissipation due to viscous flow within the magma on a one hand, and the energy dissipation due to brittle failure and uplift of the overburden on the other hand. This model shows that high-viscosity magma, such as felsic magmas, favors intrusions with higher T/D aspect ratios, which are necessarily associated with more inelastic damage and faulting in the overburden (Fig 9, Stage 3,

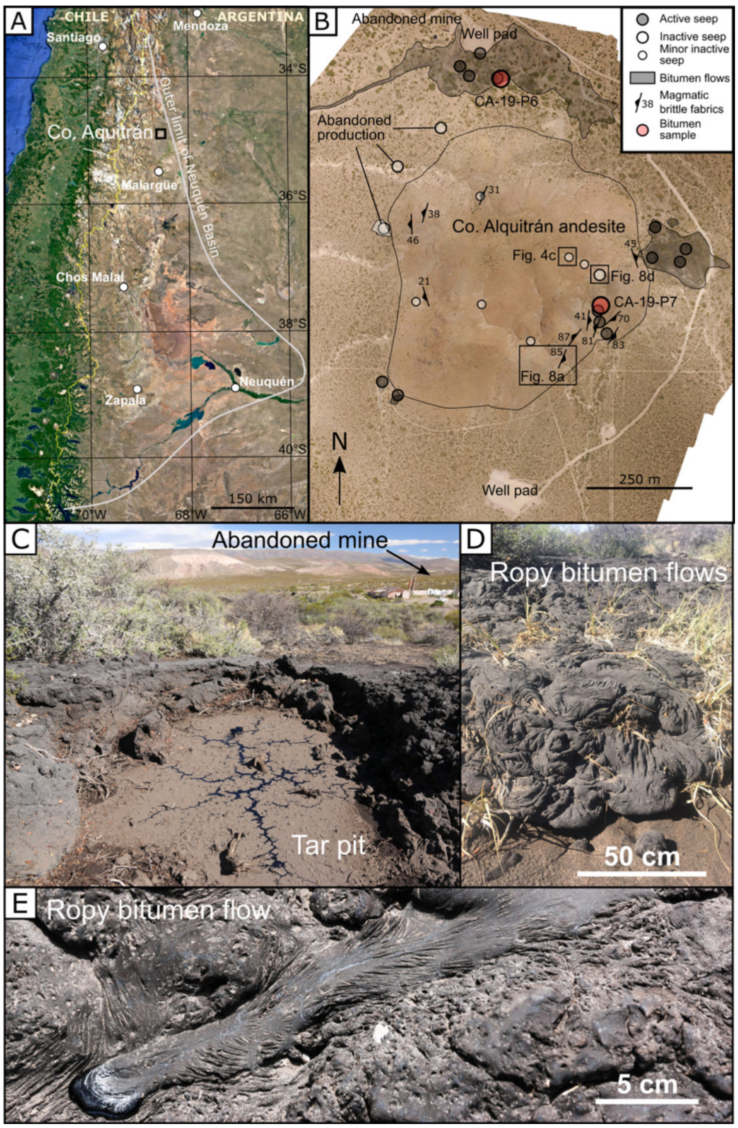

Figure 10. A. Landsat image locating the study area, on the northern part of the Neuquén Basin. Location map, north of Malargüe. B. Orthorectified image of Cerro Alquitrán computed from photographs shot from drone survey. Map displays major active and inactive seeps, and minor inactive seeps, that cluster around and within the igneous body. It displays also structural measurements of brittle magmatic fabric. C-E. Characteristic manifestations of bitumen seep at Cerro Alquitrán. C. Tar pit. D. Ropy flow complex. E. Detail of ropy flow. From Galland *et al.* (in preparation).

left). Conversely, low-viscosity magma such as mafic magma can flow easily along conduits with lower T/D aspect ratios, favoring the formation of thin sills associated with little to moderate damage and faulting in the overburden (Fig 9, Stage 3, right). These theoretical predictions are in good agreement with geological observations (e.g., Delpino *et al.* 2014).

STRUCTURES WITHIN IGNEOUS INTRUSIONS: THE CERRO ALQUITRÁN CASE STUDY

Galland *et al.* (in preparation) described an outstanding geological case study in the Neuquén Basin, Argentina, that demonstrates how ancient subvolcanic intrusions deeply affect regional-scale fluid flow. This natural laboratory is an exhumed 10.7±0.5 million-year-old subvolcanic intrusion, Cerro Alquitrán, located at the foothills of the Andes mountains, Argentina (Fig. 10) (Nullo *et al.* 2002). It is an intrusion of andesitic composition emplaced through the Mesozoic and Cenozoic sedimentary formations of the northern Neuquén Basin (Boll *et al.* 2014). The shape of the intrusion is inferred to exhibit a thick laccolithic to plug shape (Dessanti 1959).

The peculiarity of Cerro Alquitrán is the presence of large natural bitumen seeps along the edges of the igneous body (Fig. 10). Note that the Cerro Alquitrán intrusion is one body out of a whole complex of subvolcanic intrusions, where other, less voluminous bitumen seeps have also been documented (Dessanti 1959).The major bitumen seeps occur in various forms, from tar pits to long bitumen flows (Fig. 10). The surface of the bitumen flows often exhibits ropy structures that mimic basaltic Pahoehoe lava flows. Several undocumented seeps have been located around the intrusion. Three old and currently inactive seeps were exploited along the western edge of the andesite body (Fig. 10)(Galland *et al.*, in preparation). A major active seep at the SW tip of the intrusion was discovered. In all these localities, the fluids seep out through the soil that covers the geological structures associated with the andesite body. Finally, new active seeps in a gully on the SE part of the intrusion were discovered, in addition to numerous minor inactive seeps in the middle of the igneous body (Fig. 10). In these latter discoveries, the bitumen seeps out directly from the magmatic rock (Fig. 10). On map view, the overall distribution of the major seeps follows the edge of the intrusion (Fig. 10), showing a clear structural relationship between the intrusion and the fluid migration pathways.

Galland *et al.* (in preparation) investigated the internal structure of the subvolcanic intrusion to reveal its relationship with the bitumen flow. The igneous body exhibits a prominent brittle fabric close to the edges of the intrusion, consisting of gentle to steep outward-dipping planes (Fig. 11). In-between these planes, the andesite rock is affected by intense fracturing perpendicular to the planes (Fig. 11). Subsequently, we will refer to these fractured domains as fracture bands (Mattsson *et al.* 2018). Locally, the fracturing is so intense that the andesite exhibits bands of brecciated material, in which kinematic indicators highlight that the inner part of the intrusion moved upward with respect to the outer part (Fig. 11). The strike directions of these bands are

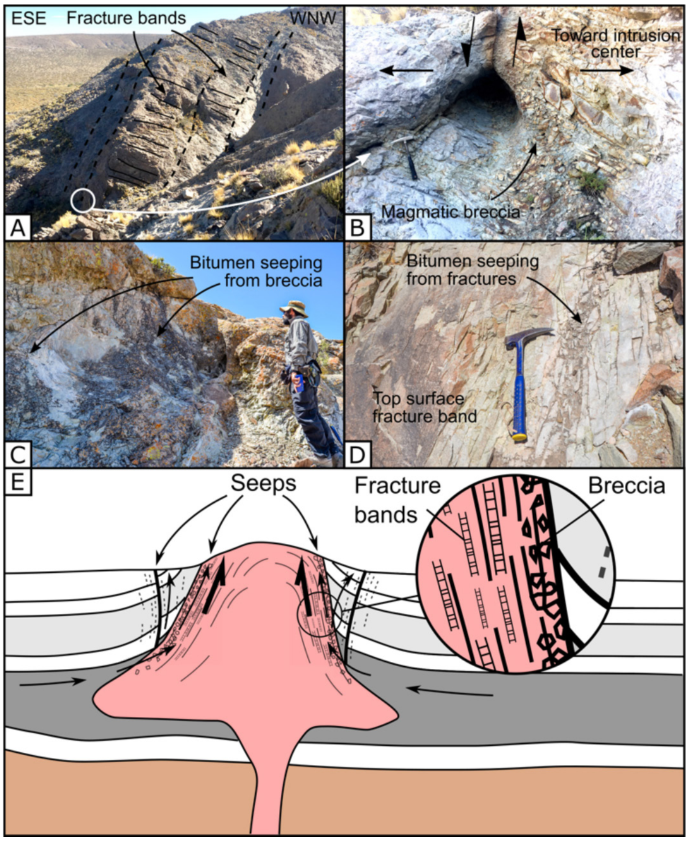

Figure 11. Characteristic structures within andesite of Cerro Alquitrán (see locations in Figure 10). A. Strongly outward-dipping fracture bands (delimited by dashed lines), with intense fracturing perpendicular to the bands. B. Sub-vertical breccia with fault gauge indicating upward movement of the interior of the intrusion. C. Bitumen seeping out from breccia zone. D. Sup surface of fracture band showing intense fracturing and local bitumen seep from fractures. E. Schematic model of structure of Cerro Alquitrán intrusive and its implications for hydrocarbon migration. From Galland *et al.* (in preparation).

overall concentric (Fig. 11). These observations suggest that the structural grain in the igneous body results from syn-emplacement brittle deformation of the magma. Close to the intrusion's contacts, shearing of the andesite was such that the deformation mode crossed the ductile-brittle transition, i.e. the andesite could not flow but was instead deforming by breaking (Cordonnier *et al.* 2012; Pistone *et al.*2015). Very similar structures have been observed at other exhumed felsic intrusions (Mattsson *et al.* 2018; Burchardt *et al.* 2019) and felsic active volcanic conduits (Lavallée *et al.* 2008; Hornby *et al.* 2019). The concentric distribution of the brittle flow fabric confirms that Cerro Alquitrán is a steep-sided laccolithic intrusion (Fig. 11). The steeper fabric and the presence of breccia bands along the SE flank of the intrusion suggests that the intrusive body was asymmetrical, with intense strain localization along the SE flank. Finally, the shallowing of the fabric toward the inner parts of the body indicates that the exposed level is likely close to the paleo-roof of the intrusion (Fig. 11).

Galland *et al.* (in preparation) observed in the field that the syn-emplacement brittle structures are the main pathways for the bitumen migration. In the SE gully, the bitumen seeps out from sub-vertical breccia bands and dense fracture bands (Fig. 11). The breccia bands appear aligned with seep lines, subparallel to the intrusion's edge. Locally, the porosity within the breccia and parts of the fracture bands is impregnated with bitumen. The syn-emplacement brittle structures of the andesite, therefore, act as the main primary pathways for bitumen migration (Fig. 11). Geological observations reveal how extinct subvolcanic intrusions have long-term consequences on subsurface fluid circulations in volcanic basins (Galland *et al.*, in preparation).

FRACTURING PROCESSES ASSOCIATED WITH SILLS EMPLACED IN ORGANIC-RICH SHALE

Rabbel *et al.* (2021) provide a very detailed field study of the fracturing processes and associated fracture distribution in an igneous petroleum system consisting of andesite sills emplaced in organic-rich shale. The studied outcrop is located at El Manzano, southern Mendoza province. It is the exposed equivalent of the Los Cavaos, Los Volcanoes, and Río Grande oil fields, where sills are fractured reservoirs (Rabbel *et al.* 2018; Spacapan *et al.* 2020). A proper understanding of the reservoir properties requires a solid description of fracture types and their distribution within the petroleum system.

The result of the fracture mapping is summarized in Figure 12 (Rabbel *et al.* 2021). The conclusions are listed in the following paragraphs:

- Four different fracture types present in sills, driven by a broad spectrum of physical processes, were identified. These include (1) cooling joints created by thermal contraction, (2) faults and associated tectonic fractures, (3) bitumen dykes and bituminous shale injection structures, and (4) hydrothermal veins, likely due to hydrofracturing initiated in the metamorphic aureole.
- Except for tectonic fractures, the fracture network is established during the early phase of magma cooling, dominated by a high-temperature environment. Evidence shows that in this phase, generated hydrocarbons may be mobilized and migrate into the intrusion and experience temperatures of several hundreds of degrees, where in-situ combustion of volatiles and graphitization of solid bitumen takes place.
- The different fracture types are observed throughout the outcrop, but they do not occur spatially homogenous. Instead, the fracture network properties exhibit strong lateral changes on the scale of some tens to hundreds of meters, depending on the number and intensity of processes involved. Local fracture pattern variations seem to be correlated with local morphological features of the intrusions, such as steps between intrusive segments, showing that a detailed knowledge of intrusion shapes is key for assessing

fracture distribution variability. Such changes involve locally increased fracture density, wider orientation distribution, higher connectivity and a variable length distribution.

- Comparison of different mathematical distributions of fractures within the intrusions, i.e. cooling joints, shows that fracture lengths are best represented through a spatially varying log-normal distribution, although even this is not overall satisfactory. The analysis also demonstrates that previously suggested power-law behavior is very unlikely and difficult to justify considering the various physical processes at work.

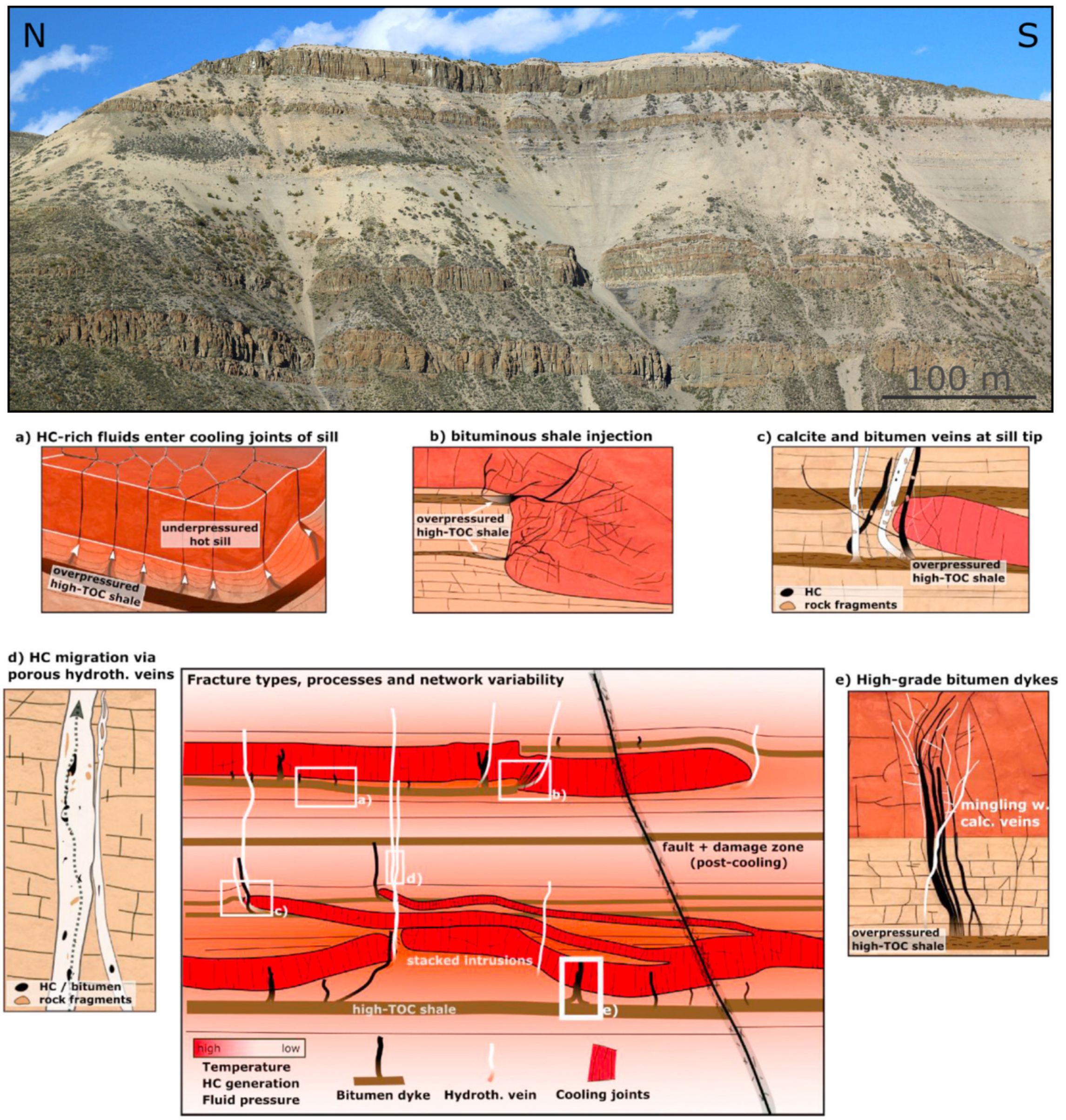

Figure 12. Top. Field photograph of part of the El Manzano outcrop (Rabbel *et al.* 2018; Rabbel *et al.* 2021), exposing andesitic sills (brown cliffs) emplaced into organic-rich shale. Bottom. Schematic summary of fracture types, underlying mechanisms and fracture network variations interpreted from field evidence presented in this paper. Central image visualizes the large-scale features, including intrusion architecture and its relation to spatial fracture network variations. Insets (a–f) highlight specific fracture types and potential implications for igneous reservoirs. From Rabbel *et al.* (2021)

- Bitumen-filled fractures in the host rock result from fast maturation of the organic matter contained in the host organic-rich shale. The fast generation of hydrocarbons in the very low-permeability rocks triggers large fluid pressure build up, which leads to the growth a connected fracture network (Kobchenko *et al.* 2013; Kobchenko *et al.* 2014; Rabbel *et al.* 2020). This contact metamorphic process is expected only if the host rock is an organic-rich shale Fm., but very unlikely in other host rock lithologies (Townsend *et al.* 2015; Galerne and Hasenclever 2019).
- Strong variations in fracture network properties imply similar heterogeneities for petrophysical and geophysical properties, such as locally enhanced storage capacity and fracture permeability or reduced seismic velocities.

Overall, the study of Rabbel *et al.* (2021) extends our understanding of fracture networks in igneous intrusions acting as petroleum reservoirs and provides numerous field examples and quantitative data. The El Manzano field analogue can thus be used to help geoscientists of all disciplines to better constrain modeling efforts and develop a more practical understanding of subsurface igneous petroleum systems.

CONCLUDING REMARKS

This review highlights that igneous intrusions have tremendous mechanical and structural impacts on sedimentary formations, with implications for fluid flow at various scales. The structural impacts are related to both syn-emplacement and post-emplacement of igneous intrusions, and at different scales. The following paragraphs summarize these processes.

Syn-emplacement, within the intrusion: syn-emplacement fracturing and brecciation of the magma, especially of felsic composition, can create high-permeability pathways along the margins of intrusions;

Syn-emplacement, in the host rock, small scale: damage and rock failure induced by the propagation of intrusion tips. Distinct modes of propagations lead to distinct damage distributions.

Syn-emplacement, in the host rock, large scale: the growth of sills and laccoliths trigger uplift and doming of their overburden. Whether this doming occurs by elastic bending or by inelastic faulting has major consequences on fluid trap of on the development of fractured reservoirs.

Post-emplacement, in the host rock and intrusion: cooling of intrusions leads to the development of cooling fractures, the distribution and connectivity of which is greatly influenced by the detailed shapes of intrusions, with major consequences for igneous fractured reservoirs. Conversely, the heating of organic-rich shale in metamorphic aureoles around cooling sills lead to fast maturation of the organic matter, fluid pressure build-up, and in situ growth of fracture network transporting hydrocarbon. Such fractures can lead to the injection of large bitumen dykes.

This review summaries our understanding of the mechanical and structural implications of igneous intrusions, and lists the main structural and mechanical aspects to address when exploring hydrocarbons in the near vicinity of igneous intrusions emplaced in hydrocarbon-bearing basins.

ACKNOWLEDGEMENTS

The laboratory models and the fieldwork at Las Loicas were funded by the DIPS project (grant 240767) from the Research Council of Norway. The fieldwork at Pampa Amarilla was funded by ROCH S.A. The authors thank ROCH S.A. for access to subsurface data and approval of publishing part of the data. The fieldwork at Cerro Alquitrán was funded through a Småforsk grant deliverd by the Department of Geosciences, University of Oslo.

REFERENCES

Abdelmalak, M.M., Bulois, C., Mourgues, R., Galland, O., Legland, J.B., Gruber, C., 2016. Description of new dry granular materials of variable cohesion and friction coefficient: Implications for laboratory modeling of the brittle crust. Tectonophysics 684, pp. 39-51, https://doi.org/10.1016/j.tecto.2016.03.003.

Abdelmalak, M.M., Mourgues, R., Galland, O., Bureau, D., 2012. Fracture mode analysis and related surface deformation during dyke intrusion: Results from 2D experimental modelling. Earth and Planetary Science Letters 359-360, pp. 93-105, 10.1016/j.epsl.2012.10.008.

Agirrezabala, L.M., 2015. Syndepositional forced folding and related fluid plumbing above a magmatic laccolith: Insights from outcrop (Lower Cretaceous, Basque-Cantabrian Basin, western Pyrenees). Geological Society of America Bulletin, 10.1130/b31192.1.

Barrionuevo, M., Giambiagi, L., Mescua, J., Suriano, J., de la Cal, H., Soto, J.L., Lossada, A.C., 2019. Miocene deformation in the orogenic front of the Malargüe fold-and-thrust belt (35°30'–36° S): Controls on the migration of magmatic and hydrocarbon fluids. Tectonophysics, https://doi.org/10.1016/j.tecto.2019.06.005.

Bermúdez, A., Delpino, D.H., 2008. Concentric and radial joint systems within basic sills and their associated porosity enhancement, Neuquén Basin, Argentina. Geological Society, London, Special Publications 302, 185, 10.1144/SP302.13.

Boll, A., Alonso, J., Fuentes, F., Vergara, M., Laffitte, G.A., Villar, H.J., 2014. Factores controlantes de las acumulaciones de hidrocarburos en el sector norte de la Cuenca Neuquina, antre los Ríos Diamante y Salado, Provincia de Mendoza, Argentina, in: IX Congreso de Exploración y Desarrollo de Hidrocarburos, Book Factores controlantes de las acumulaciones de hidrocarburos en el sector norte de la Cuenca Neuquina, antre los Ríos Diamante y Salado, Provincia de Mendoza, Argentina, Edition ed. Series, pp. 3-44.

Bunger, A.P., Cruden, A.R., 2011. Modeling the growth of laccoliths and large mafic sills: Role of magma body forces. Journal of Geophysical Research 116, B02203, 10.1029/2010jb007648.

Burchardt, S., Mattsson, T., Palma, J.O., Galland, O., Almqvist, B., Mair, K., Jerram, D.A., Hammer, Ø., Sun, Y., 2019. Progressive Growth of the Cerro Bayo Cryptodome, Chachahuén Volcano, Argentina—Implications for Viscous Magma Emplacement. Journal of Geophysical Research: Solid Earth 124, pp. 7934-7961, 10.1029/2019JB017543.

Cartwright, J., Hansen, D.M., 2006. Magma transport through the crust via interconnected sill complexes. Geology 34, pp. 929-932.

Cameron, R., González, J.M., Schiuma, M., 2002. Los reservorios de las rocas igneas intrusivas, in: V Congreso de Exploración y Desarrollo de Hidrocarburos, Book Los reservorios de las rocas igneas intrusivas, Edition ed. Series, Instituto Argentino del Petroleo y del Gas, pp. 559-582.

Cordonnier, B., Caricchi, L., Pistone, M., Castro, J., Hess, K.-U., Gottschaller, S., Manga, M., Dingwell, D.B., Burlini, L., 2012. The viscous-brittle transition of crystal-bearing silicic melt: Direct observation of magma rupture and healing. Geology 40, pp. 611-614, 10.1130/g3914.1.

Corry, C.E., 1988. Laccoliths; mechanisms of emplacement and growth.

Cruden, A.R., McCaffrey, K.J.W., Bunger, A.P., 2018. Geometric Scaling of Tabular Igneous Intrusions: Implications for Emplacement and Growth, in: Breitkreuz, C., Rocchi, S. (Eds.), Physical Geology of Shallow Magmatic Systems: Dykes, Sills and Laccoliths. Springer International Publishing, Cham, pp. 11-38.

de la Cal, H., Feinstein, E., Villar, H., 2018. Origen de los petróleos alojados en rocas ígneas intruidas en la Formación Vaca Muerta del yacimiento Cajón de los Caballos, provincia de Mendoza, Cuenca Neuquina, Argentina, in: Sánchez, M., Frydman, M., Hryb, D. (Eds.), X Congreso de Exploración y Desarrollo de Hidrocarburos. Instituto Argentino del Petroleo y del Gas, Mendoza, pp. 315-328.

Delpino, D., Bermúdez, A., Vitulli, N., Loscerbo, C., 2014. Sistema de petróleo no convencional relacionado con lacolitos eocenos de intraplaca. Área Altiplanicie del Payún, Cuenca Neuquina, in: IX Congreso de Exploración y Desarrollo de Hidrocarburos, Book Sistema de petróleo no convencional relacionado con lacolitos eocenos de intraplaca. Área Altiplanicie del Payún, Cuenca Neuquina, Edition ed. Series, Argentinean Oil and Gas Institute (IAPG), pp. 223-242.

Dessanti, R.N., 1959. Geologia del Cerro Alquitran y alrededores, Departamento de San Rafael (Prov. de Mendoza). Museo de La Plata, Notas XIX, Geología 71, pp. 301-325.

Fuentes, F., Horton, B.K., Starck, D., Boll, A., 2016. Structure and tectonic evolution of hybrid thick- and thin-skinned systems in the Malargüe fold–thrust belt, Neuquén basin, Argentina. Geological Magazine 153, pp. 1066-1084, 10.1017/S0016756816000583.

Galerne, C.Y., Hasenclever, J., 2019. Distinct Degassing Pulses During Magma Invasion in the Stratified Karoo Basin—New Insights From Hydrothermal Fluid Flow Modeling. Geochemistry, Geophysics, Geosystems 20, pp. 2955-2984, https://doi.org/10.1029/2018GC008120.

Galland, O., Bertelsen, H.S., Eide, C.H., Guldstrand, F., Haug, Ø.T., Leanza, H.A., Mair, K., Palma, O., Planke, S., Rabbel, O., Rogers, B.D., Schmiedel, T., Souche, A., Spacapan, J.B., 2018. Storage and transport of magma in the layered crust-Formation of sills and related flat-lying intrusions, in: Burchardt, S. (Ed.), Volcanic and Igneous

Plumbing Systems. Elsevier, pp. 111-136.

Galland, O., Cobbold, P.R., Hallot, E., de Bremond d'Ars, J., Delavaud, G., 2006. Use of vegetable oil and silica powder for scale modelling of magmatic intrusion in a deforming brittle crust. Earth and Planetary Science Letters 243, pp. 786-804.

Galland, O., de la Cal, H., Mescua, J., Rabbel, O., 2022. 3-dimensional trapdoor structure of laccolith-induced doming and implications for laccolith emplacement, Pampa Amarilla, Mendoza Province, Argentina. Tectonophysics, 229418, https://doi.org/10.1016/j.tecto.2022.229418.

Galland, O., Mescua, J., Villar, H.J., Medialdea, A., Zanella, A., Leanza, H.A., KJerram, D.A., Planke, S., in preparation. An igneous conduit erupting petroleum: the Cerro Alquitrán, Neuquén Basin, Argentina. Geology.

Galland, O., Scheibert, J., 2013. Analytical model of surface uplift above axisymmetric flat-lying magma intrusions: Implications for sill emplacement and geodesy. Journal of Volcanology and Geothermal Research 253, pp. 114-130, http://dx.doi.org/10.1016/j.jvolgeores.2012.12.006.

Galland, O., Spacapan, J.B., Rabbel, O., Mair, K., Soto, F.G., Eiken, T., Schiuma, M., Leanza, H.A., 2019. Structure, emplacement mechanism and magma-flow significance of igneous fingers – Implications for sill emplacement in sedimentary basins. Journal of Structural Geology 124, pp. 120–135, https://doi.org/10.1016/j.jsg.2019.04.013.

González, P.D., Aragón, E., 2000. El Cerro Bayo de la Sierra Negra, Neuquén: ejemplo de un lacolito tipo Arbol de Navidad. Revista de la Asociacion Geologica Argentina 55, pp. 363-377.

Guldstrand, F., Souche, A., Bertelsen, H.S., Zanella, A., Galland, O., submitted. Emplacement of laboratory igneous sheets and fingers influenced by the Mohr-Coulomb properties of the host. Geochemistry Geophysics Geosystems.

Hornby, A.J., Lavallée, Y., Kendrick, J.E., De Angelis, S., Lamur, A., Lamb, O.D., Rietbrock, A., Chigna, G., 2019. Brittle-Ductile Deformation and Tensile Rupture of Dome Lava During Inflation at Santiaguito, Guatemala. Journal of Geophysical Research: Solid Earth 124, pp. 10107-10131, https://doi.org/10.1029/2018JB017253.

Jackson, M.D., Pollard, D.D., 1990. Flexure and faulting of sedimentary host rocks during growth of igneous domes, Henry Mountains, Utah. Journal of Structural Geology 12, pp. 185-206.

Kobchenko, M., Hafver, A., Jettestuen, E., Galland, O., Renard, F., Meakin, P., Jamtveit, B., Dysthe, D.K., 2013. Drainage fracture networks in elastic solids with internal fluid generation. Europhysics Letters 102, 66002, 10.1209/0295-5075/102/66002.

Kobchenko, M., Hafver, A., Jettestuen, E., Renard, F., Galland, O., Jamtveit, B., Meakin, P., Dysthe, D.K., 2014. Evolution of a fracture network in an elastic medium with internal fluid generation and expulsion. Physical Review E 90, 052801.

Lavallée, Y., Meredith, P.G., Dingwell, D.B., Hess, K.U., Wassermann, J., Cordonnier, B., Gerik, A., Kruhl, J.H., 2008. Seismogenic lavas and explosive eruption forecasting. Nature 453, pp. 507-510, 10.1038/nature06980.

Magee, C., Jackson, C.A.L., Schofield, N., 2014. Diachronous sub-volcanic intrusion along deep-water margins: insights from the Irish Rockall Basin. Basin Research 26, pp. 85-105, 10.1111/bre.12044.

Magee, C., Muirhead, J.D., Karvelas, A., Holford, S.P., Jackson, C.A.L., Bastow, I.D., Schofield, N., Stevenson, C.T.E., McLean, C., McCarthy, W., Shtukert, O., 2016. Lateral magma flow in mafic sill complexes. Geosphere 12, pp. 809-841, 10.1130/ges01256.1.

Mattsson, T., Burchardt, S., Almqvist, B.S.G., Ronchin, E., 2018. Syn-Emplacement Fracturing in the Sandfell Laccolith, Eastern Iceland–Implications for Rhyolite Intrusion Growth and Volcanic Hazards. Frontiers in Earth Science 6, 10.3389/feart.2018.00005.

Nullo, F.E., Stephens, G.C., Otamendi, J., Baldauf, P.E., 2002. El volcanismo del Tertiario superior del sur de Mendoza. Revista de la Asociación Geológica Argentina 57, pp. 119-132.

Orchuela, I., Lara, M.E., Suarez, M., 2003. Productive Large Scale Folding Associated with Igneous Intrusions: El Trapial Field, Neuquen Basin, Argentina, in: AAPG International Conference, Book Productive Large Scale Folding Associated with Igneous Intrusions: El Trapial Field, Neuquen Basin, Argentina, Edition ed. Series.

Petford, N., Cruden, A.R., McCaffrey, K.J.W., Vigneresse, J.L., 2000. Granite magma formation, transport and emplacement in the Earth's crust. Nature 408, pp. 669-673.

Pistone, M., Cordonnier, B., Caricchi, L., Ulmer, P., Marone, F., 2015. The Viscous to Brittle Transition in Crystal- and Bubble-Bearing Magmas. Frontiers in Earth Science 3, https://doi.org/10.3389/feart.2015.00071.

Plazibat, S., Rasgido, A., Paredes, J.M., 2019. Subsurface characterization of Cenozoic igneous activity at Cerro Dragón area (Golfo San Jorge Basin, central Patagonia): Implications for basin evolution and hydrocarbon prospectivity. Journal of South American Earth Sciences 96, 102389, https://doi.org/10.1016/j.jsames.2019.102389.

Pollard, D.D., 1973. Derivation and evaluation of a mechanical model for sheet intrusions. Tectonophysics 19, pp. 233-269, http://dx.doi.org/10.1016/0040-1951(73)90021-8.

Pollard, D.D., Johnson, A.M., 1973. Mechanics of growth of some laccolithic intrusions in the Henry Mountains, Utah, II. Bending and failure of overburden layers and sill formation. Tectonophysics 18, pp. 311-354.

Pollard, D.D., Muller, O.H., Dockstader, D.R., 1975. The Form and Growth of Fingered Sheet Intrusions. Geological Society of America Bulletin 86, pp. 351-363, 10.1130/0016-7606(1975)86<351:tfagof>2.0.co;2.

Rabbel, O., Galland, O., Mair, K., Lecomte, I., Senger, K., Spacapan, J.B., Manceda, R., 2018. From field analogues to realistic seismic modelling: a case study of an oil-producing andesitic sill complex in the Neuquén Basin, Argentina. Journal of the Geological Society, 10.1144/jgs2017-116.

Rabbel, O., Mair, K., Galland, O., Grühser, C., Meier, T., 2020. Numerical Modeling of Fracture Network Evolution in Organic-Rich Shale With Rapid Internal Fluid Generation. Journal of Geophysical Research: Solid Earth 125, e2020JB019445, https://doi.org/10.1029/2020JB019445.

Rabbel, O., Palma, J.O., Mair, K., Galland, O., Spacapan, J.B., Senger, K., 2021. Fracture networks in shale-hosted igneous intrusions: Processes, distribution and implications for igneous petroleum systems. Journal of Structural Geology 150, 104403, https://doi.org/10.1016/j.jsg.2021.104403.

Rodriguez Monreal, F., Villar, H.J., Baudino, R., Delpino, D., Zencich, S., 2009. Modeling an atypical petroleum system: A case study of hydrocarbon generation, migration and accumulation related to igneous intrusions in the Neuquén Basin, Argentina. Marine and Petroleum Geology 26, pp. 590-605, http://dx.doi.org/10.1016/j.marpetgeo.2009.01.005.

Rossello, E.A., Cobbold, P.R., Diraison, M., Arnaud, N., 2002. Auca Mahuida (Neuquén basin, Argentina): A Quaternary shield volcano on a hydrocarbon-producing substrate, in: 5th ISAG, Extended Abstracts, Book Auca Mahuida (Neuquén basin, Argentina): A Quaternary shield volcano on a hydrocarbon-producing substrate, Edition ed. Series, pp. 549-552.

Scheibert, J., Galland, O., Hafver, A., 2017. Inelastic deformation during sill and laccolith emplacement: insights from an analytic elasto-plastic model. Journal of Geophysical Research: Solid Earth 122, pp. 923-945, 10.1002/2016JB013754.

Schiuma, M., Llambías, E.J., 2014. Importancia de los sills como reservorios en la Cuenca Neuquina del sur de Mendoza, in: IX Congreso de Exploración y Desarrollo de Hidrocarburos, Book Importancia de los sills como reservorios en la Cuenca Neuquina del sur de Mendoza, Edition ed. Series, IAPG, Trabajos Técnicos I, pp. 331-349.

Schmiedel, T., Galland, O., Breitkreuz, C., 2017a. Dynamics of sill and laccolith emplacement in the brittle crust: role of host rock strength and deformation mode. Journal of Geophysical Research: Solid Earth 122, pp.8860-8871, 10.1002/2017JB014468.

Schmiedel, T., Galland, O., Haug, Ø.T., Dumazer, G., Breitkreuz, C., 2019. Coulomb failure of Earth's brittle crust controls growth, emplacement and shapes of igneous sills, saucer-shaped sills and laccoliths. Earth and Planetary Science Letters 510, pp. 161-172, https://doi.org/10.1016/j.epsl.2019.01.011.

Schmiedel, T., Kjoberg, S., Planke, S., Magee, C., Galland, O., Schofield, N., Jackson, C.A.-L., Jerram, D.A., 2017b. Mechanisms of overburden deformation associated with the emplacement of the Tulipan sill, mid-Norwegian margin. Interpretation 5, SK23-SK38, 10.1190/int-2016-0155.1.

Schofield, N., Brown, D.J., Magee, C., Stevenson, C.T., 2012. Sill morphology and comparison of brittle and non-brittle emplacement mechanisms. Journal of the Geological Society 169, pp. 127-141, 10.1144/0016-76492011-078.

Senger, K., Millett, J., Planke, S., Ogata, K., Eide, C.H., Festøy, M., Galland, O., Jerram, D.A., 2017. Effects of igneous intrusions on the petroleum system: a review. First break 35, pp. 47-56, 10.3997/1365-2397.2017011.

Spacapan, J.B., D'Odorico, A., Palma, O., Galland, O., Rojas Vera, E., Ruiz, R., Leanza, H.A., Medialdea, A., Manceda, R., 2020. Igneous petroleum systems in the Malargüe fold and thrust belt, Río Grande Valley area, Neuquén Basin, Argentina. Marine and Petroleum Geology 111, pp. 309-331, https://doi.org/10.1016/j.marpetgeo.2019.08.038.

Spacapan, J.B., Galland, O., Leanza, H.A., Planke, S., 2017. Igneous sill and finger emplacement mechanism in shale-dominated formations: a field study at Cuesta del Chihuido, Neuquén Basin, Argentina. Journal of the Geological Society 174, pp. 422-433, 10.1144/jgs2016-056.

Spacapan, J.B., Palma, O., Galland, O., Manceda, R., Rocha, E., D'Odorico, A., Leanza, H.A., 2018. Thermal impact of igneous sill complexes on organic-rich formations and the generation of a petroleum system: case study in the Neuquén Basin, Argentina. Marine and Petroleum Geology 91, pp. 519-531, https://doi.org/10.1016/j.marpetgeo.2018.01.018.

Townsend, M., Pollard, D.D., Johnson, K., Culha, C., 2015. Jointing around magmatic dikes as a precursor to the development of volcanic plugs. Bulletin of Volcanology 77, pp. 1-13, 10.1007/s00445-015-0978-z.

Trude, J., Cartwright, J., Davies, R.J., Smallwood, J., 2003. New technique for dating igneous sills. Geology 31, pp. 813-816.

Ventsel, E., Krauthammer, T., 2002. Thin Plates and Shells: Theory, Analysis, and Applications. Applied Mechanics Reviews 55, B72-B73, 10.1115/1.1483356.

Wilson, P.I.R., McCaffrey, K.J.W., Wilson, R.W., Jarvis, I., Holdsworth, R.E., 2016. Deformation structures associated with the Trachyte Mesa intrusion, Henry Mountains, Utah: Implications for sill and laccolith emplacement mechanisms. Journal of Structural Geology 87, pp. 30-46, http://dx.doi.org/10.1016/j.jsg.2016.04.001.

Witte, J., Bonora, M., Carbone, C., Oncken, O., 2012. Fracture evolution in oil-producing sills of the Rio Grande Valley, northern Neuquén Basin, Argentina. AAPG Bulletin 96, pp. 1253-1277, 10.1306/10181110152.